Supporting Information

Electrocatalytic Oxygen Reduction by a Co/Co3O4@N-doped Carbon Composite Material Derived from the Pyrolysis of ZIF-67/Poplar Flowers

Yanling Wu [1], Yanmin Wang [1], Zuoxu Xiao [2], Miantuo Li [1], Yongling Ding [1], Mei-li Qi [1,*]

[1] School of Transportation and Civil Engineering, Shandong Jiaotong University, Ji'nan 250357, China;

[2] College of Science, China University of Petroleum (East China), Qingdao 266580, China;

[*] Corresponding author, E-mail: beauty0507@163.com

Material characterization

Laboratory powder X-ray diffraction patterns were collected for the samples on a Rigaku Ultima IV X-ray diffractometer with Cu Kα source (40 kV, 40 mA). The morphology and structure of the samples were observed on field-emission scanning electron microscope (FE-SEM, Quant 250FEG) equipped with energy-dispersive X-ray (EDX) detector and high-resolution transmission electron microscopy at an acceleration voltage of 200 kV (TEM, JEM-2100F). Micromeritics Belsorp-max analyzer was applied to measure the Brunauer Emmett Teller (BET) surface area and pore size distribution (PSD). X-ray photoelectron spectroscopic (XPS) measurements were conducted on an Axis Ultra instrument from Kratos using monochromatic Al Kα radiation. Raman scattering spectra were recorded on a laser Raman microscope system (Nanophoton RAMANtouch) with an excitation wavelength of 532 nm.

Electrochemical measurements

All electrochemical measurements were carried out by using a standard three-electrode configuration on a Gamry (RDE710) electrochemical workstation, where the Ag/AgCl (KCl-saturated) electrode and a carbon rod were used as reference and counter electrodes, respectively. To ensure the repeatability of the experiment, the working electrode for each of the four catalysts was prepared by using under uniform condition. The procedure for the preparation of a working electrode was as following: the catalyst powder (5 mg) was dispersed in 0.8 mL of ethyl alcohol with 40 μL of Nafion solution (5 wt %, Sigma-Aldrich) under sonication to obtain a homogeneous suspension. Then, the catalyst ink (10 μL, 0.30 $mg \cdot cm^{-2}$) was droped on the glass carbon electrode surface. For ORR tests, Cyclic voltammetry (CV) curves were collected in a N_2-saturated or O_2-saturated

0.1 M KOH electrolyte at a scan rate of 50 $mV \cdot s^{-1}$. Additionally, the activity for ORR was also evaluated *via* the RDE method by LSV from 0.2 to 1 V in O_2-saturated 0.1 M KOH electrolyte. The ORR stability in O_2-saturated 0.1 M KOH solution was tested by current versus time (i-t) test with a rotating speed of 1600 rpm. The ORR performance of the as-prepared catalysts were make a comparison with the state-of-the-art commercial Pt/C (20 wt%) electrocatalyst (HiSPEC®3000, Alfa Aesar).

Supplementary figures

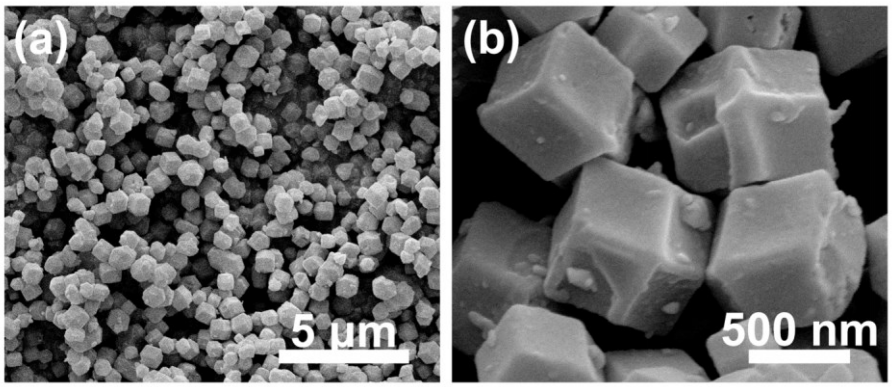

Figure S1. Representative FE-SEM images of the ZIF-67 precursor.

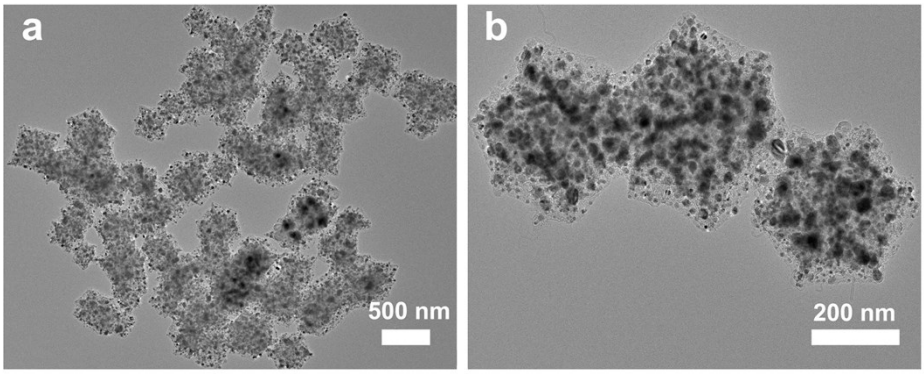

Figure S2. TEM image of the individual layer of Co@NC.

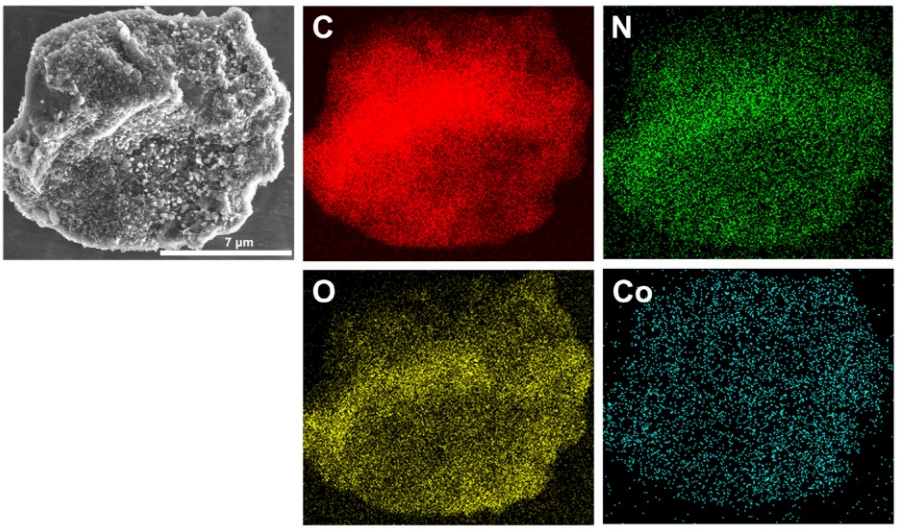

Figure S3. FE-SEM image of Co/Co_3O_4@NC used in the EDS mapping area revealing the elemental distribution of C, N, O, and Co.

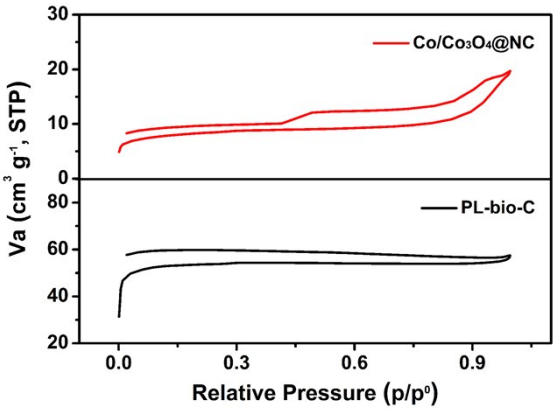

Figure S4. N_2 adsorption/desorption isotherms plot of PL-bio-C and Co/Co_3O_4@NC, respectively.

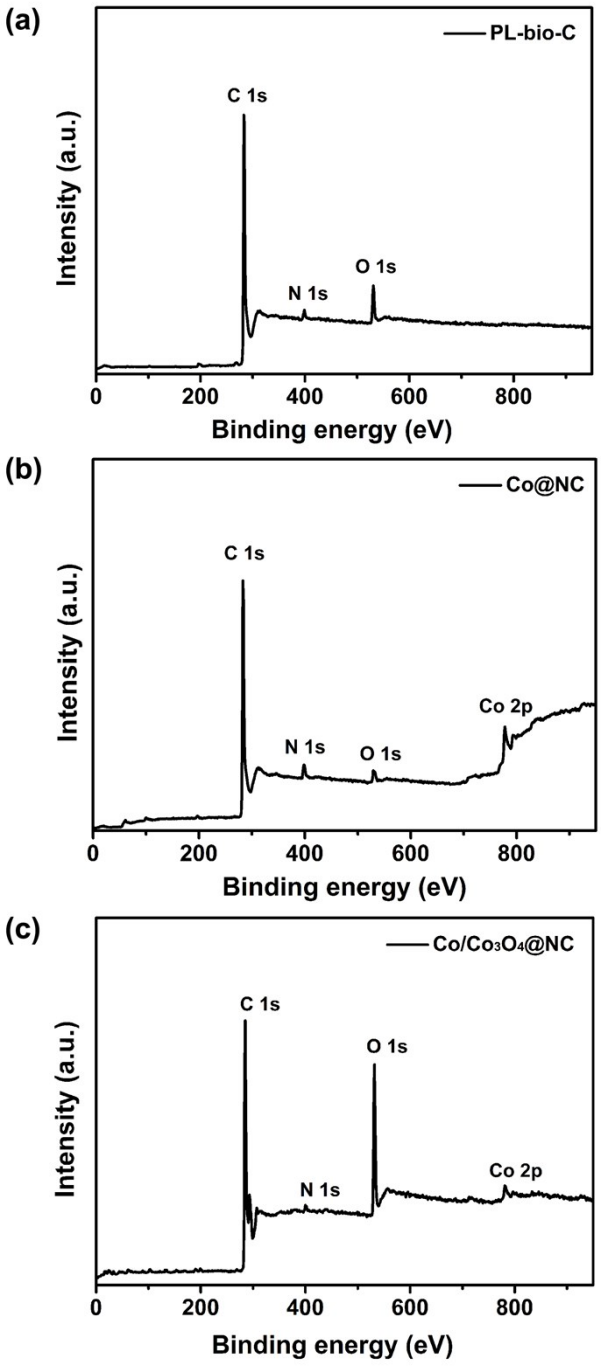

Figure S5. XPS survey spectrum of PL-bio-C, Co@NC, and Co/Co_3O_4@NC.

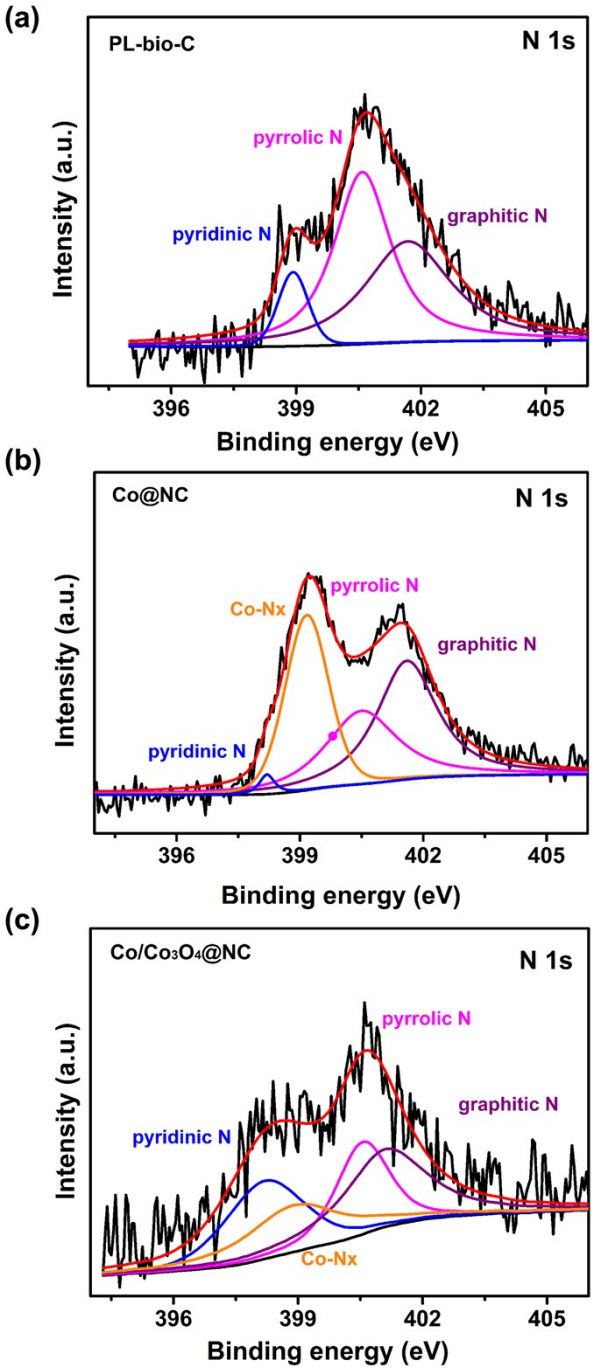

Figure S6. N 1s XPS spectra of PL-bio-C, Co@NC, and Co/Co_3O_4@NC.

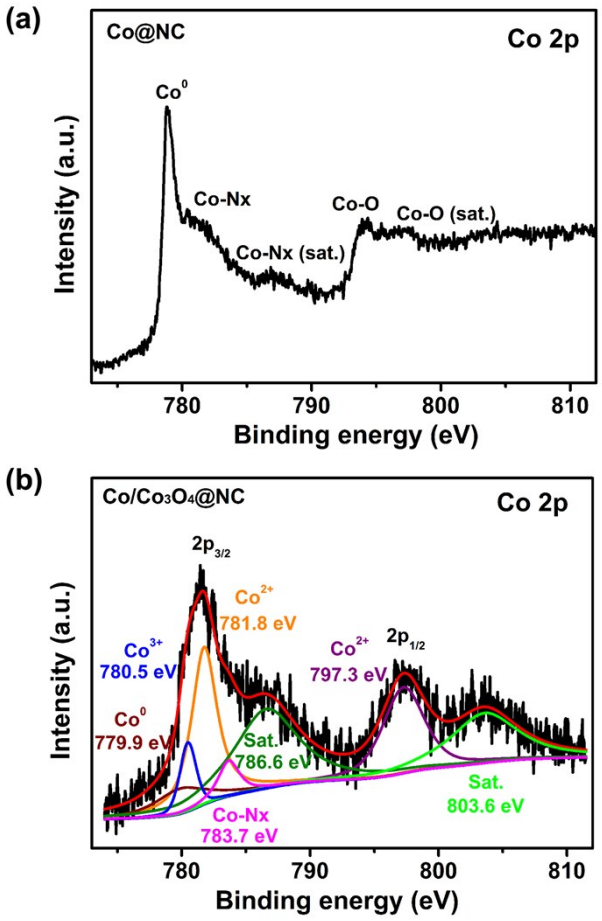

Figure S7. Co 2p XPS spectra of Co@NC, and Co/Co_3O_4@NC.

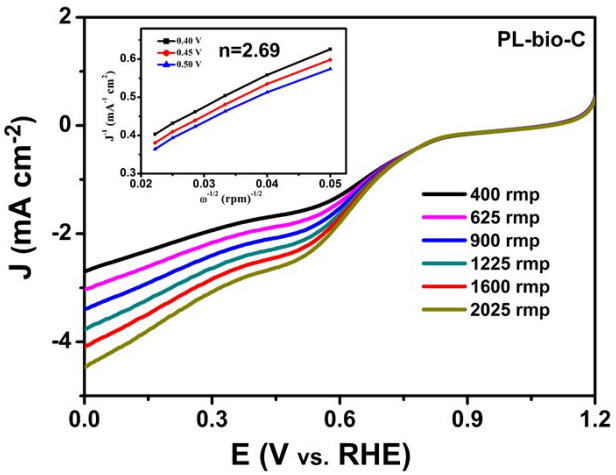

Figure S8. LSV curves of PL-bio-C catalyst at various rotating speeds. (Inset: K–L plots of PL-bio-C at various potentials.)

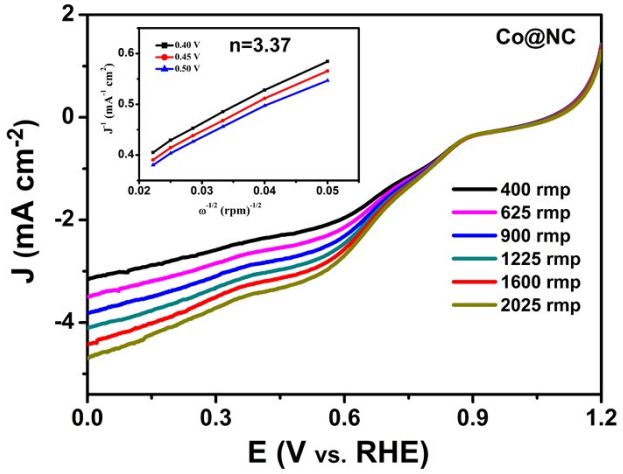

Figure S9. LSV curves of Co@NC catalyst at various rotating speeds. (Inset: K–L plots of Co@NC at various potentials.)

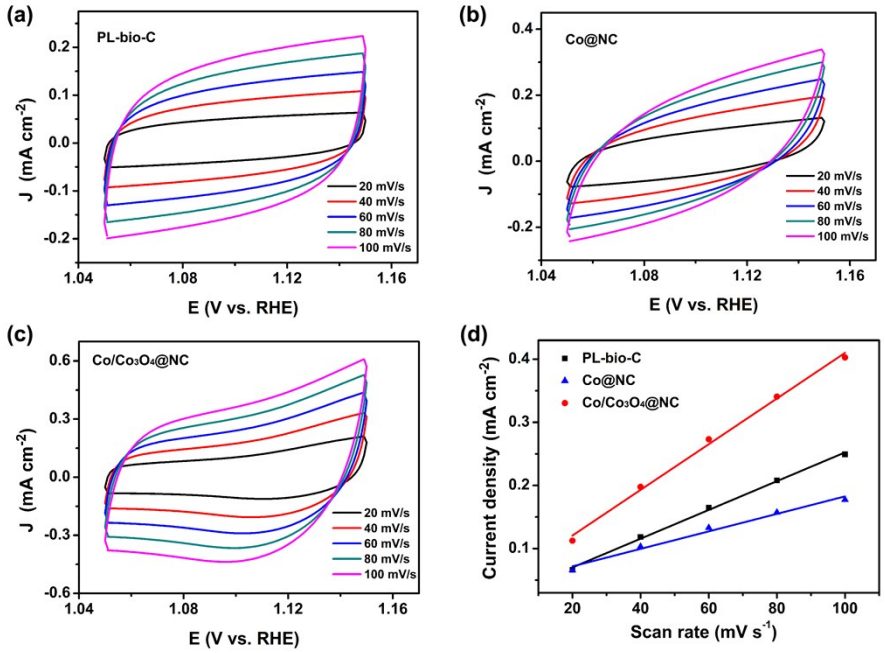

Figure S10. Cyclic voltammograms (CV) at various scan rates of (a) PL-bio-C, (b) Co@NC and (c) Co/Co_3O_4@NC in 0.1 M KOH solution. (d) The electrochemical double-layer capacitance (C_{dl}) of PL-bio-C, Co@NC, and Co/Co_3O_4@NC in 0.1 M KOH electrolyte.

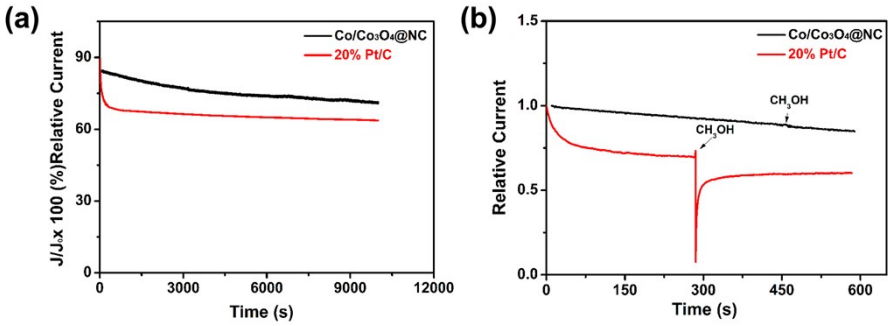

Figure S11. (a) Amperometric i–t curves of Co/Co_3O_4@NC and 20 wt% Pt/C and (b) upon the addition of 3 M methanol in O_2-saturated 0.1 M KOH solution with the rotation speed of 1600 rpm.

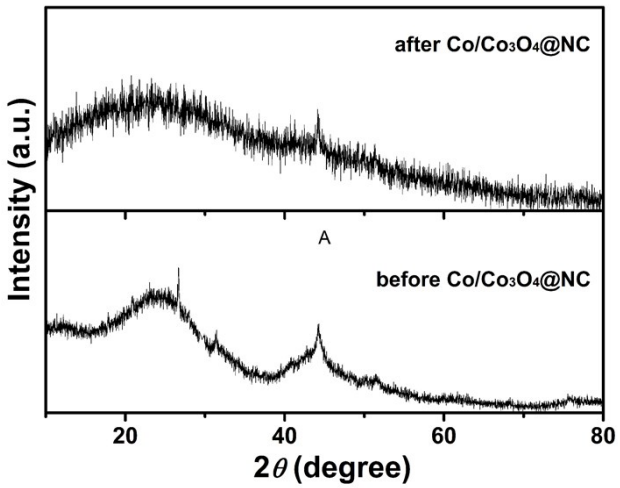

Figure S12. PXRD patterns of Co/Co_3O_4@NC catalyst before and after stability tests.

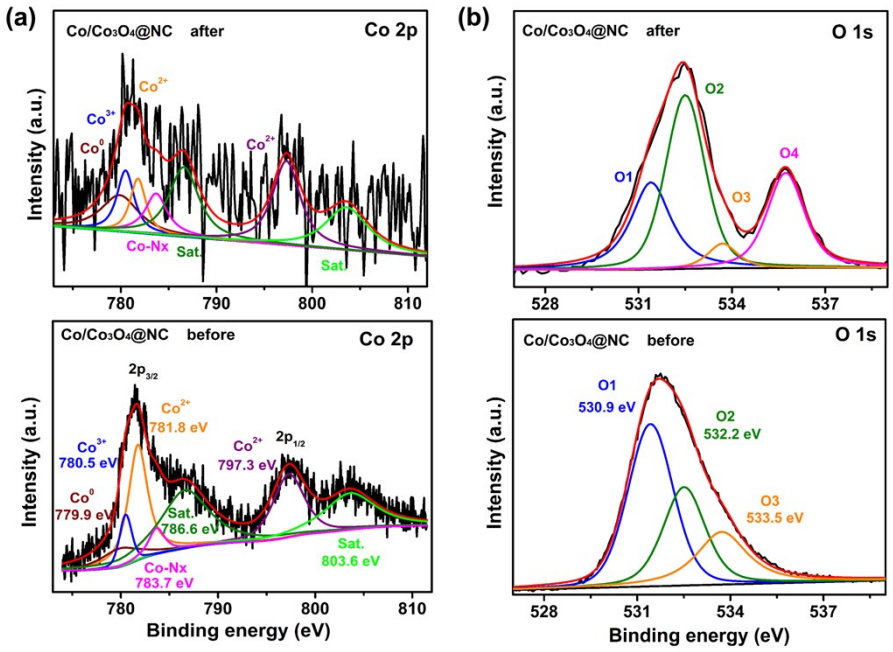

Figure S13. High-resolution XPS curves of the (a) Co 2p, and (b) O 1s core levels for Co/Co_3O_4@NC catalyst before and after stability tests.

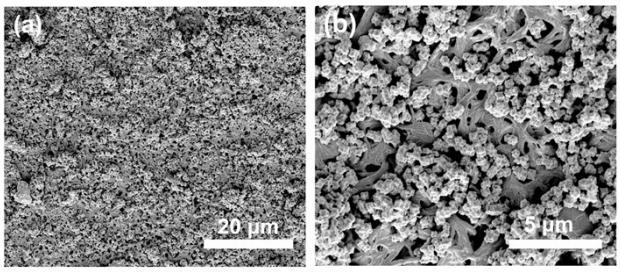

Figure S14. SEM images of Co/Co_3O_4@NC catalyst after stability tests.

Table S1. The physical parameters of the PL-bio-C and Co/Co_3O_4@NC, respectively.

Sample	Surface area (m^2 g^{-1})	Average pore diameter (nm)	Pore volume (cm^3 g^{-1})
PL-bio-C	201.43	1.74	0.087
Co/Co_3O_4@NC	30.38	3.29	0.029

Table S2. The ORR performance of the PL-bio-C. Co@NC, Co/Co_3O_4@NC and 20 wt% Pt/C in alkaline media at 1600 rpm, respectively.

Sample	E_{onset} (V)	$E_{1/2}$ (V)	J_L (mA cm^{-2})	n
PL-bio-C	0.81	0.63	3.30	2.69
Co@NC	0.87	0.68	3.86	3.37
Co/Co_3O_4@NC	0.94	0.85	4.78	3.82
20 wt% Pt/C	0.96	0.86	5.61	4.00

Table S3. Comparison of the ORR performance for Co/Co_3O_4@NC catalysts at 1600 rpm in 0.1 M KOH.

Catalysts	$E_{1/2}$ (V)	J_L (mA cm^{-2})	E_{onset} (V)	Tafel slope (mV dec^{-1})	*n*	Reference
Co/Co_3O_4@NC	0.85	4.78	0.94	90	3.82	This work
Co/Co_3O_4/C–N		3.75			3.4~3.9	*Nano Energy*, 2014 [1]
$Co@Co_3O_4$@C	0.78	4.65	0.90	--	--	*Energy Environ. Sci.*, 2015 [2]
ZIF/rGO-700-AL	0.81	5.49	0.93	--	3.77~3.97	*J. Mater. Chem. A*, 2015 [3]
Co@NG-acid	0.83	4.00	0.90	--	3.90	*Adv. Funct. Mater.*, 2016 [4]
$Co@Co_3O_4$@PPD	0.78	4.20	0.90	--	3.78~3.96	*Small*, 2016 [5]
ZIF/rGO-700-AL	0.81	5.49	0.93	--	--	*J. Mater. Chem. A*, 2016 [6]
Co@NCNT	0.83	6.20	1.03	--	--	*J. Mater. Chem. A*, 2016 [7]
Co,N-CNF	0.85	5.71	0.92	60	4.00	*Adv. Mater.*, 2016 [8]
Cal-CoZIF-VXC72	0.84	5.92	--	35	4.00	*Adv. Mater.*, 2017 [9]
Co_3O_4/Co-N-C	0.91	5.10	0.98	68.5	3.62	*Journal of Power Sources*, 2017 [10]
Co/NPC	0.79	5.46	0.91	--	3.85~4.00	*J Mater Sci*, 2018 [11]
Co_3O_4/Co@N-G	0.81	5.20	0.96	--	3.91~3.96	*J. Mater. Chem. A*, 2019 [12]
Co100@nCNFs	0.70	3.80	0.87	--	3.95	*Nanoscale Adv.*, 2019 [13]
Co-CoO-Co_3O_4/NC	0.80	5.12	0.92	--	3.91	*Electrochimica Acta*, 2019 [14]
Co_3O_4/N-ACCNF	0.79	5.60	0.98	--	4.0	*Inorg. Chem. Front.*, 2019 [15]
Co/Co_3O_4@NHCS	0.82	5.00	0.95	76.6	3.88~3.98	*Materials Today Energy*, 2020 [16]
Co-Co_3O_4@NAC	0.795	6.2	0.935	--	3.8	*Applied Catalysis B: Environmental*, 2020 [17]

References

(1) Wu, Z. Y.; Chen, P.; Wu, Q. S.; Yang, L. F.; Pan, Z.; Wang, Q. Co/Co_3O_4/C–N, a novel nanostructure and excellent catalytic system for the oxygen reduction reaction. *Nano Energy* **2014**, 8, 118–125.

(2) Xia, W.; Zou, R. Q.; An, L.; Xia, D. G.; Guo, S. J. Metal-organic framework route to in-situ encapsulation of Co@Co_3O_4@C core@bishell nanoparticles into highly ordered porous carbon matrix for oxygen reduction. *Energy Environ. Sci.* **2015**, 8, 568–576.

(3) Wei, J.; Hu, Y. X.; Wu, Z. X.; Liang, Y.; Leong, S.; Kong, B.; Zhang, X. Y.; Zhao, D. Y.; Simon, G. P.; Wang, H. T. A graphene-directed assembly route to hierarchically porous Co–Nx/C catalysts for high performance oxygen reduction. *J. Mater. Chem.* A **2015**, 3, 16867–16873

(4) Zeng, M.; Liu, Y. L.; Zhao, F. P.; Nie, K. Q.; Han, N.; Wang, X. X.; Huang, W. J.; Song, X. N.; Zhong, J.; Li, Y. G. Metallic cobalt nanoparticles encapsulated in nitrogen enriched graphene shells: Its bifunctional electrocatalysis and application in Zinc–Air batteries. *Adv. Funct. Mater.* **2016**, 26, 4397–4404.

(5) Wang, Z. j.; Li, B.; Ge, X. M.; Thomas Goh, F. W.; Zhang, X.; Du, G. J.; Wu, D.; Liu, Z. L.; Andy Hor, T. S.; Zhang, H.; Zong, Y. Co@Co_3O_4@PPD core@bishell nanoparticle-based composite as an efficient electrocatalyst for oxygen reduction reaction. *Small* **2016**, 12, 2580–2587.

(6) Wei, J.; Hu, Y. X.; Wu, Z. X.; Liang, Y.; Leong, S.; Kong, B.; Zhang, X. Y.; Zhao, D. Y.; Simon, G. P.; Wang, H. T. A graphene-directed assembly route to hierarchically porous Co-Nx/C catalysts for high performance oxygen reduction. *J. Mater. Chem. A* **2015**, 3, 16867–16873.

(7) Zhang, E.; Xie, Y.; Ci, S. Q.; Jia, J. C.; Cai, P. W.; Yi, L. C.; Wen, Z. H. Multifunctional high-activity and robust electrocatalyst derived from metal-organic frameworks. *J. Mater. Chem. A* **2016**, 4, 17288–17298.

(8) Shang, L.; Yu, H. J.; Huang, X.; Bian, T.; Shi, R.; Zhao, Y. F.; Waterhouse, G. I. N.; Wu, L. Z.; Tung, C. H.; Zhang, T. R. Well-dispersed ZIF-derived Co,N-Co-doped carbon nanoframes through mesoporous-silica-protected calcination as efficient oxygen reduction electrocatalysts. *Adv. Mater.* **2016**, 28, 1668–1674.

(9) Ni, B.; Ouyang, C.; Xu, X. B.; Zhuang, J.; Wang, X. Modifying commercial carbon with trace amounts of ZIF to prepare derivatives with superior ORR

activities. *Adv. Mater.* **2017**, 29, 1701354.
(10) Li, J. S.; Zhou, Z.; Liu, K.; Li, F. Z.; Peng, Z. G.; Tang, Y. G.; Wang, H. Y. Co_3O_4/Co-N-C modified ketjenblack carbon as an advanced electrocatalyst for Al-Air batteries. *J Power Sources* **2017**, 343, 30–38.
(11) Zhan, T. R.; Lu, S. S.; Rong, H. Q.; Hou, W. G.; Teng, H. N.; Wen, Y. H. Metal-organic-framework-derived Co/nitrogen-doped porous carbon composite as an effective oxygen reduction electrocatalyst. *J Mater Sci* **2018**, 53, 6774–6784.
(12) Guo, J.; Gadipelli, S.; Yang, Y. C.; Li, Z. N.; Lu, Y.; Brett, D. J. L.; Guo, Z. X. An efficient carbon-based ORR catalyst from low temperature etching of ZIF-67 with ultra-small cobalt nanoparticles and high yield. *J. Mater. Chem. A* **2019**, 7, 3544–3551.
(13) Khalily, M. A.; Patil, B.;Yilmaz, E.; Uyar, T. Atomic layer deposition of Co_3O_4 nanocrystals on N-doped electrospun carbon nanofifibers for oxygen reduction and oxygen evolution reactions. Nanoscale Adv. **2019**, 1, 1224–1231.
(14) Yi, X. R.; He, X. B.; Yin, F. X.; Chen, B. H.; Li, G. R.; Yin, H. Q. Co-CoO-Co_3O_4/N-doped carbon derived from metal-organic framework: The addition of carbon black for boosting oxygen electrocatalysis and Zn-Air battery. Electrochim Acta **2019**, 295, 966–977.
(15) Qiu, L. Z.; Han, X. P.; Lu, Q.; Zhao, J.; Wang, Y.; Chen, Z. L.; Zhong, C.; Hu, W. B.; Deng, Y. D. Co_3O_4 nanoparticles supported on N-doped electrospinning carbon nanofifibers as an efficient and bifunctional oxygen electrocatalyst for rechargeable Zn-air batteries. Inorg. Chem. Front. **2019**, 6, 3554–3561.
(16) Wang, X. K.; Gai, H. Y.; Chen, Z. K.; Liu, Y. H.; Zhang, J. J.; Zhao, B. L.; Toghan, A.; Huang, M. H. The marriage of crystalline/amorphous Co/Co_3O_4 heterostructures with N-doped hollow carbon spheres: efficient and durable catalysts for oxygen reduction. Mater Today Energy. **2020**, 18, 100497.
(17) Zhong, X. W., Yi, W. D.; Qu ,Y. J.; Zhang, L. Z.; Bai, H. Y.; Zhu, Y. M.; Wan, J.; Chen, S.; Yang, M.; Huang, L.; Gu, M.; Pan, H.; Xu, B. M. Co single-atom anchored on Co_3O_4 and nitrogen-doped active carbon toward bifunctional catalyst for zinc-air batteries. Electrochim Acta **2020**, 260, 118188.